EUROfusion

EUROFUSION WPJET1-CP(16) 15097

TJJ Tala et al.

Density Peaking in JET - Driven by Fuelling or Transport?

Preprint of Paper to be submitted for publication in
Proceedings of 26th IAEA Fusion Energy Conference

This work has been carried out within the framework of the EUROfusion Consortium and has received funding from the Euratom research and training programme 2014-2018 under grant agreement No 633053. The views and opinions expressed herein do not necessarily reflect those of the European Commission.

Density Peaking in JET – Driven by Fuelling or Transport?

T. Tala[1], A. Salmi[1], C. Bourdelle[2], L. Giacomelli[3], C. Giroud[4], R. Gomes[5], J. Hillesheim[4], A. Järvinen[6], C. Maggi[4], P. Mantica[3], M. Maslov[4], L. Meneses[5], S. Menmuir[4], S. Moradi[7], S. Mordijck[8], V. Naulin[9], H. Nordman[10], J. Juul Rasmussen[9], G. Sips[11], J.L. Svensson[12], M. Tsalas[13], H. Weisen[14], A. Wynn[4] and JET contributors*

EUROfusion Consortium, JET, Culham Science Centre, Abingdon, OX14 3DB, UK
[1]VTT, P.O. Box 1000, FI-02044 VTT, Espoo, Finland
[2]CEA, IRFM, F-13108 Saint-Paul-lez-Durance, France
[3]Istituto di Fisica del Plasma, via Cozzi 53, 20125 Milano, Italy
[4]CCFE, Culham Science Centre, Abingdon, OX14 3DB, UK
[5]Instituto de Plasmas e Fusão Nuclear, IST, Universidade de Lisboa, Portugal, IST, Lisbon, Portugal
[6]Lawrence Livermore National Laboratory, US
[7]Ecole Polytechnique, CNRS UMR7648, LPP, F-91128, Palaiseau, France
[8]College of William & Mary, Virginia, USA
[9]Danish Technical University Physics, Lyngby, Denmark
[10]Chalmers University of Technology, Göteborg 41296, Sweden
[11]Commission, Brussels, Belgium
[12]IPP, Greifswald, Germany
[13]DIFFER, Nieuwegein, Netherlands
[14]CRPP, Lausanne, Switzerland
*See the author list of "Overview of the JET results in support to ITER" by X. Litaudon et al. to be published in Nuclear Fusion Special issue: overview and summary reports from the 26th Fusion Energy Conference (Kyoto, Japan, 17-22 October 2016).

Abstract. Particle transport has been extensively studied by performing several dimensionally matched collisionality scans in various plasma scenarios in JET. Gas puff modulation technique has been developed with high quality time-dependent density profile measurements to determine particle transport coefficients. Density peaking has been found to increase with decreasing υ^* in all H-mode scenarios while in L-mode, no dependency was found. The experimentally determined particle transport coefficients suggest that NBI fueling is main contributor to the observed density peaking in H-mode. This is further supported by predictive transport simulations with GLF23 and gyro-kinetic analysis. These results will extrapolate to future tokamaks in such a way that density peaking may be quite moderate even in low collisionality regimes in the absence of core particle sources.

1. Introduction

Particle transport in tokamaks has received much less attention than electron and ion heat transport channels. It is still often not treated self-consistently in transport modelling and predictions for future tokamaks. As a consequence, particle transport and fuelling have remained one of the major open questions in understanding the ITER physics [1]. The shape of the density profile has a significant influence on fusion performance and impurity transport.

Extensive database studies in JET showed that density peaking scales with several plasma parameters, the most dominant ones being collisionality υ^*, Greenwald fraction and NBI fuelling [2,3]. Collisionality was found to be the dominating parameters in JET, and this was further supported in C-Mod experiment where the core fueling is small [4]. The neutral beam fuelling source was found to be the second most important factor. On the other hand in L-mode plasmas, the plasma internal inductance li was to found to be the key factor in determining the density peaking [5]. On the other hand, while the database studies suggested the dominant role played the collisionality in peaking the density, other particle transport analysis in JET emphasise the importance of the particle sources [6,7,8]. In these papers, the NBI fueling and also the neutral particle fueling inside the pedestal are found as the most important factor in contributing to the peaking of the density profile. It was reported that the normalised density gradient depends strongly on the normalised particle flux. In addition, the particle diffusion coefficient was found to be small with respect to heat diffusivity, i.e. $D_{eff}/\chi_{e,eff} \approx 0.2$. However, to unanimously estimate the relative roles of different factors affecting density peaking, one has to separate the effect of transport and fueling from each other and look into the parametric dependences of transport coefficients.

Core particle transport has been studied in JET by performing various dimensionless collisionality scans both in H-mode and L-mode plasmas. Gas puff modulation technique was exploited to obtain particle transport coefficients. This is the first time to exploit gas puff modulation in JET with diagnostics having good time and spatial resolution. Concerning the edge particle transport, the relative role of neutral fuelling versus the inward convection at the edge plasma has so far been left an unexplored territory. Recently, a lot of work has been done on this front on JET, such as measuring edge particle transport coefficients and neutral fueling profiles, things that have never been measured before these experiments. However, this is left outside this paper and will be reported in future.

2. Gas Puff Modulation Experiment and the Analysis Technique

Gas modulation experiments in H-mode plasmas to study particle transport and sources at the plasma edge have been carried out on JET [9,10]. The local electron density response to the gas injection was measured with reflectometer and Thompson scattering diagnostics close to the midplane. Modulation amplitudes below 1% (in the core) are reliably measured thus allowing minimal plasma disturbance and the possibility to use data from multiple harmonics. In order to test the linearity of the gas puff modulation technique, the modulated gas puff rate was doubled for one of the discharges. The phase profile stayed the same while the amplitude doubled, thus giving confidence that fuelling from the gas puff modulation at this level is linear and does not perturb the plasma background transport. Therefore, in determining the transport coefficients, the assumption that the background is time-independent seems valid.

The gas puff modulation was performed with a gas valve at the top of the machine at 3Hz frequency using rectangular waveform, the rate varying from 0 to $6\times10^{22}s^{-1}$ at 30% duty cycle. Another gas injection module at the divertor location was used to keep the volume averaged density constant. Figure 1 illustrates the plasma shape and density modulation due to the gas injection for the shot no. 87420 (B_T=2.67T, I_P=2MA). The propagation of the perturbation is clearly seen in the reflectometer signal up to mid radius yielding data for up to three harmonics.

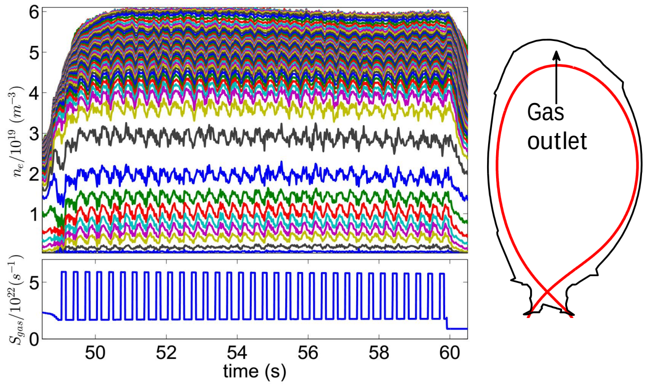

Figure 1 Experimental gas waveform and resulting density modulation. Top location (GIM7) was used for gas injection #87420.

Time resolved electron density measurements together with 1.5D transport analysis are used to clarify the mechanisms responsible for understanding the particle transport and fuelling. We assume time-independent radial profiles for the diffusion D and convection v, i.e. the plasma background is time-independent of the gas puff modulation. We are left with three unknowns, diffusion D, convection v and neutral particle source S as the NBI particle source is assumed to be known. The particle transport equation is solved using an iterative scheme where the transport coefficients and source are varied inside a non-linear optimisation routine until the simulated electron density best matches the experimental density, amplitude and phase profiles. Alternatively, one can use transport code to perform the optimization in the particle transport channel, in this paper ASTRA code has been used. More details of the scheme are given in ref. [10].

3. Dimensionless Collisionality Scans in Various JET Plasmas

The following 4 separate and independent 3-point υ^* scans were performed in JET: (i) high power ELMy H-mode featuring low β, (ii) hybrid like high β H-mode plasma, (iii) ELMy H-mode plasma in Hydrogen and (iv) L-mode with carbon wall. In each scan, roughly a factor of 5 in υ^* was achieved by scanning I_p and B_t and the NBI power. For example for the high power ELMy H-mode case (i) the scan ranged from I_p=1.7MA to 2.5 MA, B_t from 2.0T to 3.0T and the NBI power from 9MW up to 24MW, respectively. The dimensionless parameters, q, ρ^*, β_n and T_i/T_e (being very close to 1 in each of the scans presented here) were typically matched very well, for example within the H-mode scan, the difference between the shots being only a few % (<10% in worst case). This is illustrated in figure 2. Even the temperature gradient length R/L_T was constant within the scan. The rotation was not matched (increases with NBI power). The volume averaged density was very similar, within 5% between the three discharges. It is to be noted that operationally keeping density constant when scanning the plasma current to such an extent is in general far from trivial in all-metal device. The other three scans (ii), (iii) and (iv) were practically as good matches as the H-mode scan presented in figure 2.

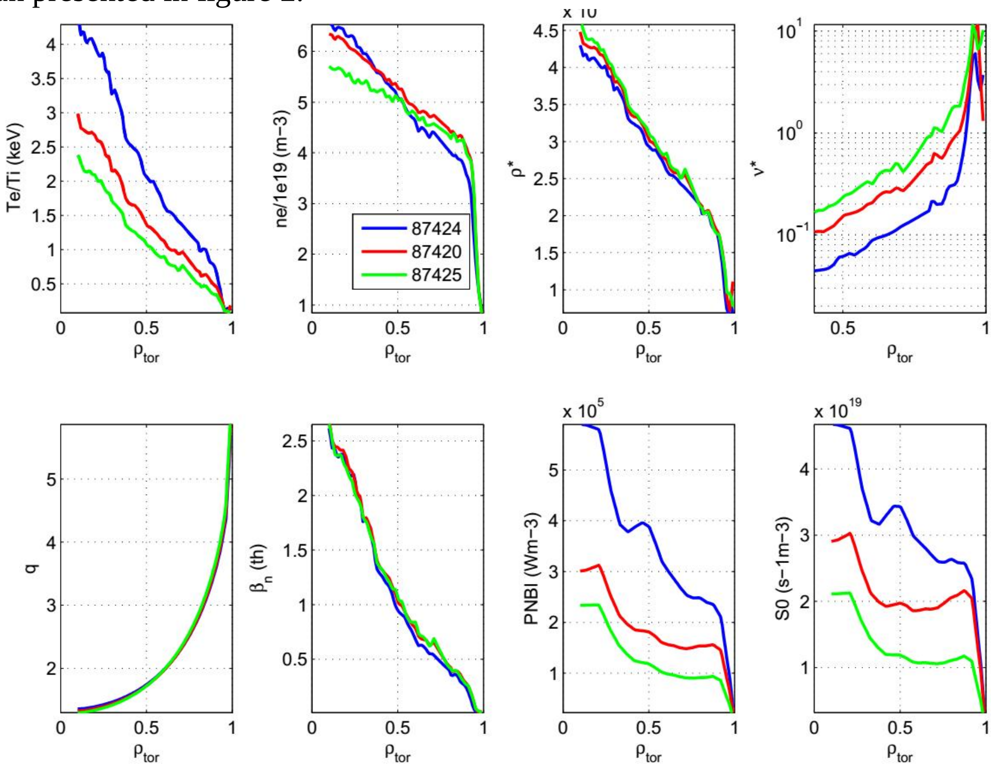

Figure 2. Profiles of temperature, density, ρ^*, υ^*, q, β, NBI power and NBI particle source for the H-mode scan (case (i)), consisting of the high collisionality shot (green, 87425), intermediate collisionality (red, 87420) and low collisionality shot (blue, 87424).

Results from the 4 different dimensionless 3-point collisionality scans with respect to density peaking are summarised in figures 3 and 4. The density profile is measured with Thomson scattering diagnostics and averaged over the stationary phase of the discharge, typically of the order of more than 5s (except in Hybrid-like plasmas). The density peaking factors are compared with the ones originating from the past database studies [3], as illustrated in figure 4. The density peaking factor is defined here as $n_e(r/a=0.2)/\langle n_e\rangle_{vol}$ i.e. density at r/a=0.2 divided by the volume averaged density.

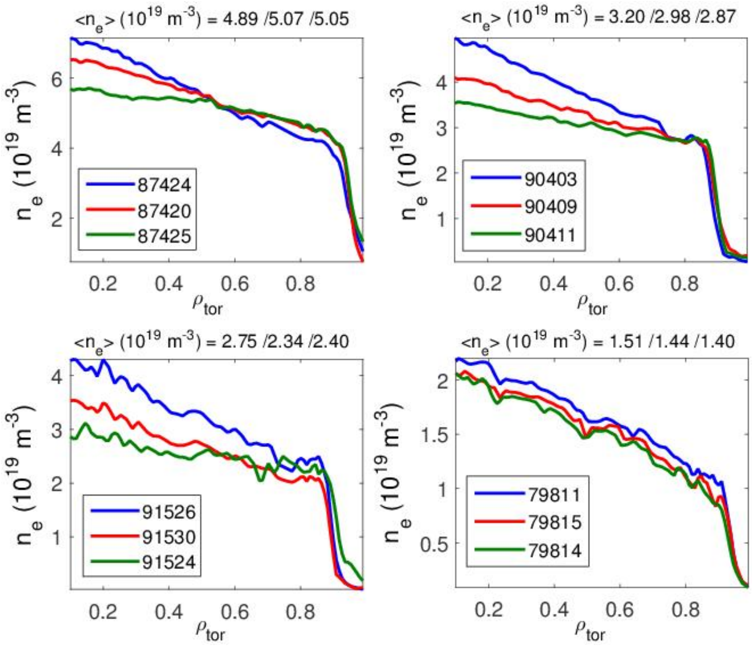

Figure 3. Density profiles from the following four different dimensionless collisionality scans: (top left, case (i)) high power ELMy H-mode featuring low β, (top right, case (ii)) hybrid like high β plasma, (bottom left, case (iii)) ELMy H-mode plasma in Hydrogen and (bottom right, case (iv)) L-mode with carbon wall. The blue colour refers to the low collisionality case and the green one to high collisionality case, the red being inbetween. The numbers on top indicate the volume averaged densities, in the order blue, red, green.

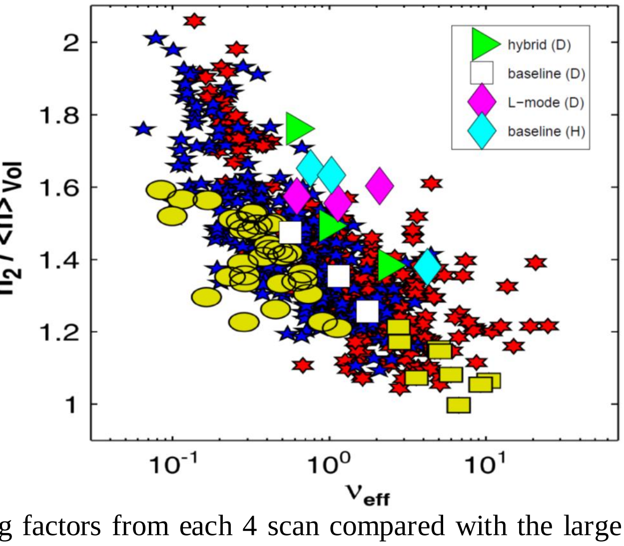

Figure 4. Density peaking factors from each 4 scan compared with the large database from [3]. The original data with blue stars from JET (NBI), red from AUG (NBI), yellow circles ICRH dominated shots from JET and yellow squares ICRH dominated shots from AUG.

The volume averaged density is very similar while the collisionality υ^* or alternatively υ_{eff} is varied simultaneously by a factor of roughly 5 within each scan. For the H-mode scan both in Deuterium (ii) and Hydrogen (iii), the peaking factor increases a short factor of 2 while υ_{eff} decreases a factor of 5 although the peaking factors are higher in Hydrogen plasmas (ii) than in Deuterium plasmas. However, the scans are not comparable to each other as q, ρ^* and β are different. In Hybrid-like plasma at higher β around 2 (it was 1.4 in the H-mode scan), the peaking increases a good factor of 2 with υ_{eff} decreasing a factor of 5. In Hybrid plasmas, density peaking is clearly highest. Looking into the same thing but with a different definition of density peaking factor, i.e. local R/Ln_e, one can note that for the H-mode case (i) it increases in the inner core (r/a=0.3) from 1.2 to 2.5 and in the outer core (r/a=0.8) from 1.5 to 3.9 when the volume averaged υ^* decreases from 0.47 to 0.09 in H-mode case. Unlike in all the different scans with H-mode plasma edge (executed with ITER-like-wall), no change in density peaking factor was observed in L-mode (carbon wall). The results from both of the dedicated H-mode and L-mode scans are consistent with the earlier density database results in L-mode [4] and H-mode [2,3] with respect to collisionality dependence of density peaking. However, here the peaking factors are located on the high side cloud of points, indicating higher peaking at a given υ_{eff}. The origin of the density peaking deserves further investigation.

4. Experimental Particle Transport Coefficients

In order to obtain the particle transport coefficients, perturbative density data from the gas puff modulation data is needed to distinguish the relative roles of fuelling versus transport. The experimental data from the gas puff modulation analysis indicates that a narrow neutral fuelling profile, peaked at the edge is most consistent with all transport analyses and thus does not significantly contribute to density peaking even at ρ=0.8 [10]. SOLPS modelling is on-going for more precise neutral source calculation and the edge particle transport analysis [11]. The 3 Hz rectangular gas modulation with ~35% duty cycle yields density perturbation above the noise level for up to 3rd harmonic.

The transport coefficients have been determined using ASTRA transport code by choosing the diffusion D and convection v in such way that the least square error between the simulated and experimental steady-state n_e, and the modulation amplitudes $A(n_e)$ and phases $\Phi(n_e)$ is minimized. This technique is analogous to the analysis method of the JET NBI modulation experiment [12]. The beam particle source is calculated with PENCIL. The results are shown in figure 5 for JET pulse 87420 which is the intermediate shot in the Deuterium H-mode collisionality scan.

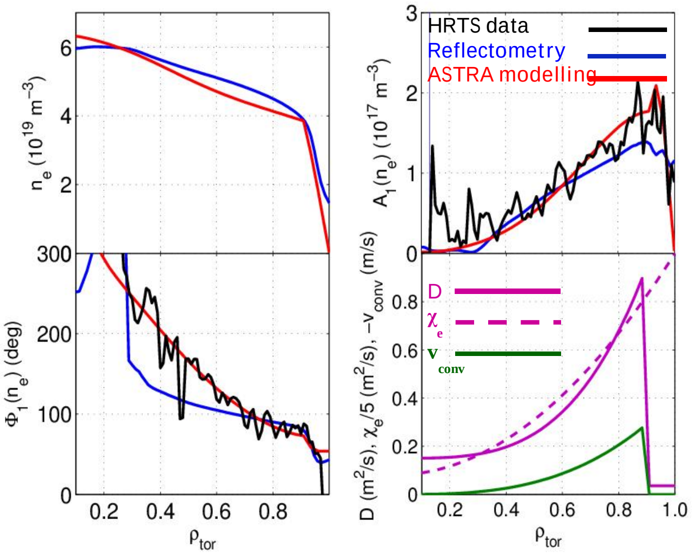

This data has the longest stationary phase, over 12s resulting in good 35 modulation cycles. Steady-state and modulation amplitude $A(n_e)$ of n_e are well reproduced with the inferred D and v, shown in the bottom right panel. Also the phase of ne modulation $\Phi(n_e)$ is well reproduced against HRTS data. The same set of D and v reproduces also the second and third harmonic data and gives thus an extra confidence on the accuracy of the analysis.

Figure 5. Determination of the particle transport coefficients for pulse no 87420.

Recently, further iterative schemes with parametrised D, v and S are begin developed exploiting non-linear optimisation routines. This will be in particular useful near the plasma edge where the recycled and puffed neutral source S remains an extra unknown quantity.

5. Transport Modelling and Gyro-kinetic Analysis the Density Peaking Pulses

The key question is what the fraction of inward convection versus NBI particle source (and possibly a little also the neutral particle source) is in contributing to the observed, relatively strong density peaking with decreasing υ^*. It is important to point out that the NBI fuelling rate increases, for example in the high power H-mode case (i), from 0.8×10^{21} 1/s to 2.3×10^{21} 1/s while υ^* decreases by a factor of 5, see figure 2 (bottom right frame).

To quantify density the origin of the peaking, the baseline ELMy H-mode scan (case (i)) has been modelled with GLF23 transport model. The simulations were performed with JETTO transport code by having T_i, T_e and n_e in a predictive mode, but using experimentally measured profiles for toroidal rotation and *q*-profile. The simulations included the *ExB* shear stabilisation. The modelling results are summarized in figure 6. The upper row shows the quality of the simulations with respect to the experimental data (solid curves) in predicting the ion (blue) and electron (red) temperature correctly for each of the three collisionalities. The prediction for the density is presented in the lower row. Two simulations are compared in each frame, one with the calculated beam particle source with PENCIL code (dashed) included and another one without the NBI source (dotted). While the predictions for the temperature profiles are not very sensitive to having or not having the NBI particle source, the predictions for the density profiles are. For the low and intermediate collisionality discharges, GLF23 predicts that approximately a half of the density peaking is due to the NBI fuelling whereas for the high υ^* case according to GLF23, the peaking is virtually all from the NBI particle source. This simulation result is consistent with the experimentally determined transport coefficients.

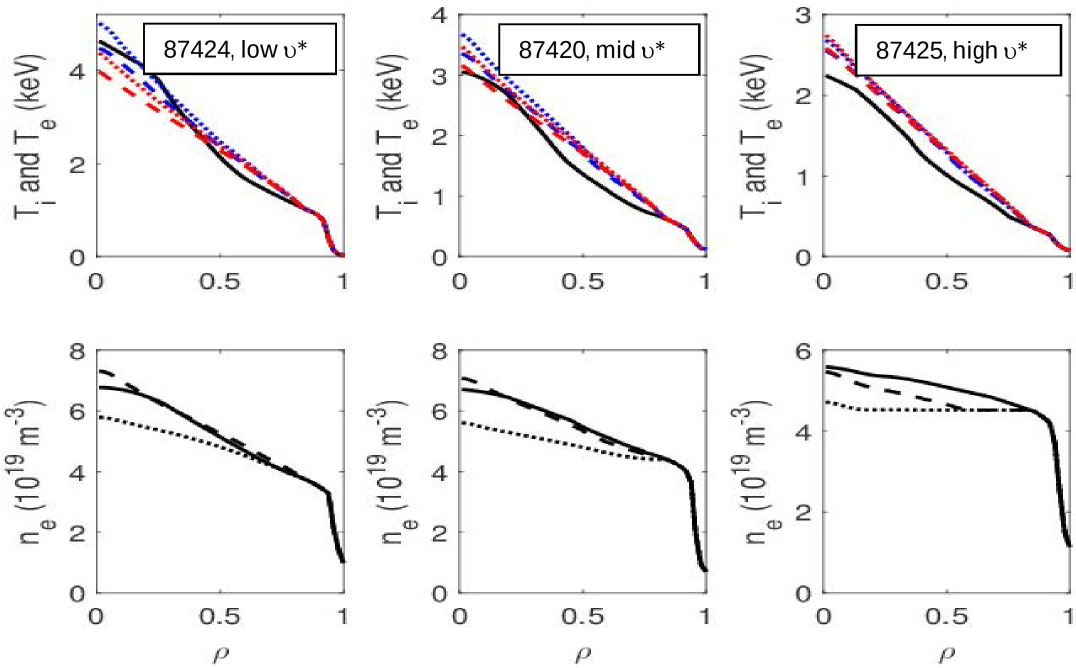

Figure 6. GLF23 transport modelling results for the ELMy H-mode baseline υ^* scan. Predictions for ion (blue) and electron (red) compared to the experiment (black solid, assuming T_e=T_i). Two simulations are compared in each frame, one with the calculated beam particle source with PENCIL (dashed) and the one without the NBI source (dotted). Lower row as in upper row, but for density predictions.

In addition to transport modelling, density peaking was performed by comparing the measured density peaking values to those ones from experimentally determined *D* and *v* for the H-mode collisionality scan (case i). This means in practice that the density peaking, due to the inferred *D* and *v* values (transport effect only), are directly compared to the measured density peaking. In addition, the density peaking factor will be compared to the linear gyro-kinetic simulations with GYRO and fluid runs with the Weiland model. Unfortunately we have so far only one shot (#87420) with thoroughly analysed transport coefficients (see section 4) which we can use in the comparison. The peaking factor caused by the determined *D* and *v* are the green triangles in figure 7. The black circles are the measured values therefore including both fueling and transport, and as can be seen, the determined *D* and v yield much smaller density peaking than the measured one. This indicates that at least for this pulse, the NBI fueling is the dominant factor contributing to density peaking. The small values of *v* and *D* would not yield such a density peaking themselves, and in fact indeed, they are both relatively small (shown in figure 5).

Additional information can be obtained from the gyro-kinetic and fluid modelling. The GYRO runs were linear, electro-magnetic, and with drift-kinetic electrons at k_y=0.3. The results turned out to be sensitive to the choice of k_y [13]. Weiland fluid runs were also done at k_y=0.3. R/L_n was searched for the root of the interpolated normalized electron flux as a function of a/L_{ne} by assuming zero particle flux.

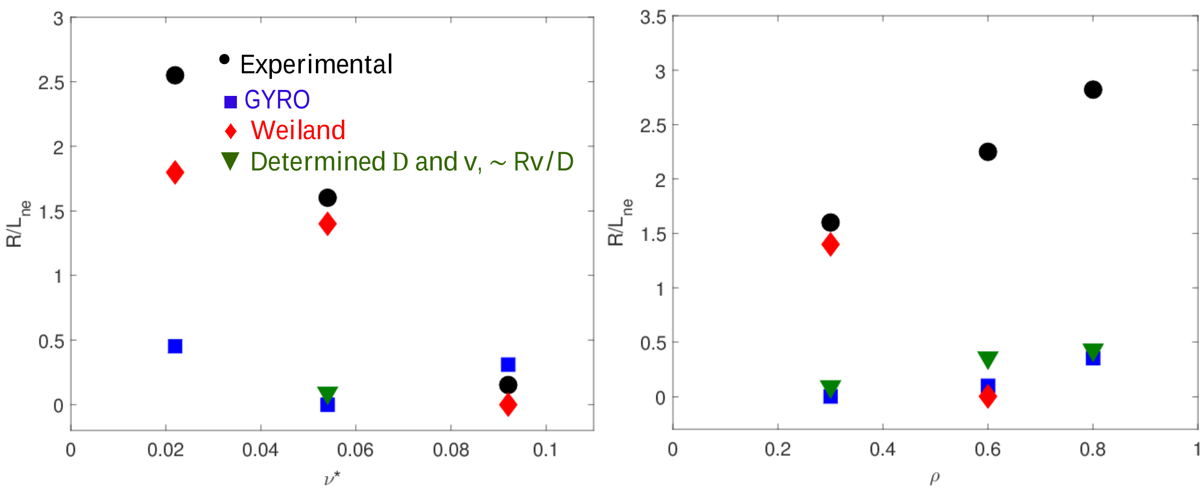

Figure 7. Left frame: Density peaking as a function of υ* from the 3-point υ* scan in baseline H-mode plasma (case i) at ρ=0.3 (#87424 at υ*=0.02, #87420 at υ*=0.06 and #87425 at υ*=0.09). Right frame: density peaking for JET pulse #87420. Both frames include the experimentally measured (black circles), experimentally determined transport coefficients (green triangle) and the modelled GYRO (blue squares) and Weiland (red diamonds) density peaking profiles.

There are two very important messages in figure 7. Firstly, the difference between the measured experimental R/L_{ne} and the ones from the determined transport coefficients that exclude the NBI fuelling contribution show that the NBI fuelling plays a major role in contributing to the density peaking (due to large difference between black and green points). For this JET discharge (#87420), fuelling is the dominant factor as the part below the green triangles are due to inward pinch and the difference between black dots and green triangles is due to NBI fuelling. Secondly, GYRO with the assumptions discussed above predicts very small values of density peaking at each collisionality –

and is in fact consistent with the determined transport coefficient for pulse 87420. The Weiland fluid model overestimates the density peaking for #87420 and gives much higher values than GYRO except at high collisionality.

6. Summary and Conclusions

Particle transport has been extensively studied by performing several dimensionally matched collisionality scans in different plasma scenarios in JET. Gas puff modulation technique has been developed in great detail with high quality density measurements to determine particle transport coefficients. Density peaking has been found to increase with decreasing υ^* in all H-mode scenarios while in L-mode, no dependency was found. However, both the experimentally determined particle transport coefficients, predictive transport simulations with GLF23 and first gyro-kinetic analysis all emphasise a significant role of the NBI fueling rather than anomalous inward convection in affecting density peaking. Similar conclusions on stressing the significance of the NBI fueling in density peaking are reported on DIII-D [14]. The resulting particle diffusion coefficient is small, i.e. $D_{eff}/\chi_{e,eff} \approx 0.2$, consistent with [8]. Under these plasma conditions performed in these scans, all the models and gyro-kinetic analyses show that transport is ITG dominated. Therefore, the anomalous pinch is quite low for all discharges under this collision dominated, for ITG/TEM turbulence, regime. In more collisionless cases, the modelling would give larger turbulent density peaking, making the extrapolation to ITER from these cases less certain.

Further work is needed to quantify these results, in particular, more pulses with long stationary gas puff modulation phase are needed to be able to see the magnitude of D and v (that results in low density peaking) presented in this paper in other plasma conditions. Moreover, additional gyro-kinetic analysis and transport modelling will be performed to see if the trends are reproducible in various scenarios and by several codes and models. The extrapolation to future tokamaks, like ITER, is the final goal here and based on these results, the density peaking may not be as high as predicted in the earlier database papers [2-4] in the absence of core particle sources.

Acknowledgement: "This work has been carried out within the framework of the EUROfusion Consortium and has received funding from the Euratom research and training programme 2014-2018 under grant agreement No 633053. The views and opinions expressed herein do not necessarily reflect those of the European Commission."

[1] A. Loarte *et al*., Nucl. Fusion **53**, 083031 (2013).
[2] H. Weisen *et al.*, Plasma Phys. Control. Fusion **48**, A457 (2006).
[3] C. Angioni *et al*., Nucl. Fusion **47** 1326–1335 (2007).
[4] M. Greenwald *et al*., Nucl. Fusion **47** L26–L29 (2007).
[5] H. Weisen et al., Plasma Phys. Control. Fusion **46**, 751 (2004).
[6] M. Valovic *et al*., Phys. Control. Fusion **46**, 1877 (2004).
[7] L. Garzotti *et al*., Nucl. Fusion **46**, 994 (2006).
[8] M. Valovic *et al*., Nucl. Fusion **47**, 196 (2007).
[9] T. Tala *et al*., 42nd EPS Conference, Lisbon, Portugal, 22-26 June 2015.
[10] A. Salmi *et al*., 42nd EPS Conference, Lisbon, Portugal, 22-26 June 2015.
[11] S. Mordijck *et al*., PSI conference, 22nd PSI Conference, Rome, Italy, 30 May – 3 June 2016.
[12] T. Tala *et al.* Phys. Rev. Lett. 102, 075001 (2009).
[13] C. Bourdelle *et al.*, Phys. Plasmas 14, 112501 (2007).
[14] S. Mordijck *et al.*, in Proc. 26th IAEA Fusion Energy Conf. 17-22 October 2016, (Kyoto, Japan, 2016).